DE GRUYTER Open Mathematics 2022; 20: 986–997

Research Article

Liangying Miao and Zhiqian He*

Hopf bifurcation and Turing instability in a diffusive predator-prey model with hunting cooperation

https://doi.org/10.1515/math-2022-0474
received June 25, 2021; accepted June 28, 2022

Abstract: In this article, we study Hopf bifurcation and Turing instability of a diffusive predator-prey model with hunting cooperation. For the local model, we analyze the stability of the equilibrium and derive conditions for determining the direction of Hopf bifurcation and the stability of the bifurcating periodic solution by the center manifold and the normal form theory. For the reaction-diffusion model, first it is shown that Turing instability occurs, then the direction and stability of the Hopf bifurcation is reached. Our results show that hunting cooperation plays a crucial role in the dynamics of the model, that is, it can be beneficial to the predator population and induce the rise of Turing instability. Finally, numerical simulations are performed to visualize the complex dynamic behavior.

Keywords: predator-prey, hunting cooperation, Turing instability, Hopf bifurcation, stability

MSC 2020: 92D25, 35K57, 35B35

1 Introduction

The predator is a population that eats another population (known as prey). The prey is the food source of the predator, and the predator dies if it does not obtain food. Modeling the interaction between preys and predators has become one of the important methods to reveal their evolution law. The mathematical model describing this interaction was first proposed to explain the oscillatory levels of certain fish catches in the Adriatic by Lotka-Volterra [1,2]. Since then, based on different biological meanings, statistical data, and experiments, a lot of predator-prey models have been proposed and studied and have become an important tool for mathematicians and biologists to learn more about nature and better protect the environment.

Cooperative hunting is a social behavior intrinsically present in many predator populations. This is a common interest among predators for successfully capturing preys compared to individual efforts. Different predators employ different strategies based on their moving abilities, social skills, communication capabilities, cognitions, prey types, and availabilities. Bailey et al. [3] reviewed different strategies taken by predators during cooperative hunting of over 40 species, including carnivores [4] (lions [5], wolves [6], African wild dogs [7], and chimpanzees [8]), birds [9], ants [10], and spiders [11].

Although there are many cooperative predators in nature, there are only a few mathematical models incorporating such a biological mechanism. To the best of our knowledge, an earlier predator-prey model with hunting cooperation has been proposed by Berec [12]. Berec found that hunting cooperation has

* **Corresponding author: Zhiqian He,** Department of Basic Teaching and Research, Qinghai University, Xining, Qinghai, 810016, P. R. China, e-mail: zhiqianhe1987@163.com
Liangying Miao: School of Mathematics and Statistics, Qinghai Nationalities University, Xining, Qinghai, 810007, P. R. China

a destabilizing effect on predator-prey dynamics. Based on the research of Berec, Alves and Hilker [13] extended the classical Lotka-Volterra model by including hunting cooperation as follows:

$$\begin{cases} \dfrac{\mathrm{d}N}{\mathrm{d}\tau} = rN\left(1 - \dfrac{N}{K}\right) - N(\beta + \alpha P)P, \\ \dfrac{\mathrm{d}P}{\mathrm{d}\tau} = eN(\beta + \alpha P)P - mP, \end{cases} \tag{1.1}$$

where N and P are prey and predator densities, respectively, r is the intrinsic growth rate of the prey, K is the carrying capacity of the prey, e is the conversion efficiency, m is the mortality rate of the predator, β is the rate of predation without hunting cooperative, and α is the cooperative coefficient. r, K, e, m, β are positive constants, and, α is a non-negative constant. If $\alpha = 0$, model (1.1) becomes a classical Lotka-Volterra model with logistic growth of the prey. For simplicity, consider dimensionless variables with the following scaling:

$$u = \frac{e\beta}{m}N, \quad v = \frac{\beta}{m}P, \quad t = m\tau,$$

model (1.1) is rewritten as follows:

$$\begin{cases} \dfrac{\mathrm{d}u}{\mathrm{d}t} = \sigma u\left(1 - \dfrac{u}{k}\right) - u(1 + av)v, \\ \dfrac{\mathrm{d}v}{\mathrm{d}t} = u(1 + av)v - v \end{cases} \tag{1.2}$$

with

$$\sigma = \frac{r}{m}, \quad k = \frac{e\beta K}{m}, \quad a = \frac{\alpha m}{\beta^2}.$$

Alves and Hilker [13] investigated the stability of equilibrium in phase plane and bifurcation diagrams of model (1.2) via numerical simulations. It is shown that for some σ and a Hopf or Bogdanov-Takens bifurcations occur. Recently, Wu and Zhao [14] studied the stability of equilibrium and the existence of Hopf bifurcations for model (1.2) via mathematical analysis.

As far as we know, reaction-diffusion equations have been widely employed to study the behavior of biological phenomena in nature. In particular, Turing [15] showed that a system of coupled reaction-diffusion equations can be used to describe patterns and forms in biological systems. Turing's theory shows that diffusion could destabilize an otherwise stable equilibrium of the reaction-diffusion system and lead to nonuniform spatial patterns. This kind of instability is usually called Turing instability. Naturally, we then consider the reaction-diffusion model corresponding to model (1.2):

$$\begin{cases} \dfrac{\partial u}{\partial t} = d_1\Delta u + \sigma u\left(1 - \dfrac{u}{k}\right) - u(1 + av)v, & x \in \Omega,\ t > 0, \\ \dfrac{\partial v}{\partial t} = d_2\Delta v + u(1 + av)v - v, & x \in \Omega,\ t > 0, \\ \dfrac{\partial u}{\partial \nu} = \dfrac{\partial v}{\partial \nu} = 0, & x \in \partial\Omega,\ t > 0, \\ u(x, 0) = u_0(x),\ v(x, 0) = v_0(x), & x \in \Omega, \end{cases} \tag{1.3}$$

where Ω is a bounded domain in $\mathbb{R}^n$ with smooth boundary $\partial\Omega$ and ν is the outward unit normal on $\partial\Omega$. d_1 and d_2 are the diffusion coefficients of u and v, respectively. The initial data $u_0(x)$, $v_0(x)$ are nonnegative smooth functions, which are not identically zero. Model (1.3) has been extensively investigated by many researchers and some interesting results have also been obtained. For example, Wu and Zhao [14] considered the stability of equilibrium and, the existence of Hopf bifurcations and Turing instability. Capone et al. in [16] proved the definitive boundedness of solutions via the existence of positive invariants and attractive sets and obtained the Turing instability. Singh and Dubey [17] investigated meticulousness in the spatial dynamics of the predator-prey model with hunting cooperation via diffusion-driven instability.

However, we note that the results in [14,16] provide no further information on the direction and stability of the Hopf bifurcation in models (1.2) and (1.3). Therefore, it may be interesting to investigate such cases. We point out that this topic has been largely discussed in the literature for the predator-prey model. Based on the aforementioned reasons, in the present article, we consider the following predator-prey model with hunting cooperation

$$\begin{cases} \dfrac{du}{dt} = \sigma u(1-u) - u(1+av)v, \\ \dfrac{dv}{dt} = u(1+av)v - v. \end{cases} \tag{1.4}$$

Using the center manifold and the normal form theory, we derive conditions for determining the direction of Hopf bifurcation and the stability of the bifurcating periodic solution. Based on the above discussions, we further investigate the following reaction-diffusion model:

$$\begin{cases} \dfrac{\partial u}{\partial t} = d_1\Delta u + \sigma u(1-u) - u(1+av)v, & x \in \Omega, t > 0, \\ \dfrac{\partial v}{\partial t} = d_2\Delta v + u(1+av)v - v, & x \in \Omega, t > 0, \\ \dfrac{\partial u}{\partial \nu} = \dfrac{\partial v}{\partial \nu} = 0, & x \in \partial\Omega, t > 0, \\ u(x,0) = u_0(x), \ v(x,0) = v_0(x), & x \in \Omega. \end{cases} \tag{1.5}$$

It is worth mentioning that we can immediately reach the direction and stability of the Hopf bifurcation in model (1.5) without any tedious calculations.

For other research studies of the predator-prey model with hunting cooperation, see [18] for cross-diffusion, see [19] for time delay, see [20,21] for discrete time; in particular, Pati et al. [20] explored bifurcation patterns, novel organized structures, and chaos in the bi-parameter space of a discrete-time predator-prey model with cooperative hunting.

This article is organized as follows. In Section 2, we investigate the existence, direction, and stability of the Hopf bifurcation in model (1.4) by the Poincaré-Andronov-Hopf bifurcation theorem. In Section 3, we first consider the Turing instability of the reaction-diffusion model (1.5) when the spatial domain is a bounded interval, and then we study the existence and direction of Hopf bifurcation and the stability of the bifurcating periodic solution. Moreover, numerical simulations are presented to verify and illustrate the theoretical results above.

2 Dynamics of the local model

In this section, we mainly discuss the existence, direction, and stability of the Hopf bifurcation in model (1.4).

It is easy to verify that (1.4) has a unique positive equilibrium $(u_c, v_c) = \left(\frac{1}{\sqrt{a\sigma}}, \frac{\sqrt{a\sigma}-1}{a}\right)$ if and only if $a > \frac{1}{\sigma}$. The Jacobian matrix of (1.4) at (u_c, v_c) is as follows:

$$J(a) = \begin{pmatrix} -\sqrt{\dfrac{\sigma}{a}} & \dfrac{-2\sqrt{a\sigma}+1}{\sqrt{a\sigma}} \\ \dfrac{\sqrt{a\sigma}(\sqrt{a\sigma}-1)}{a} & \dfrac{\sqrt{a\sigma}-1}{\sqrt{a\sigma}} \end{pmatrix}, \tag{2.1}$$

and the corresponding characteristic equation is

$$\lambda^2 - \mathrm{Tr}(a)\lambda + \mathrm{Det}(a) = 0,$$

where $\mathrm{Tr}(a) = \frac{\sqrt{a\sigma} - 1 - \sigma}{\sqrt{a\sigma}}$ and $\mathrm{Det}(a) = \frac{2(\sqrt{a\sigma} - 1)^2}{a} > 0$. By the standard linearization method, we can obtain that if $a < \frac{(1+\sigma)^2}{\sigma}$ holds, then the equilibrium (u_c, v_c) of (1.4) is locally stable.

Next, we analyze the Hopf bifurcation occurring at (u_c, v_c) by choosing a as the bifurcation parameter. Denote $a_0 = \frac{(1+\sigma)^2}{\sigma}$, then when $a = a_0$, the Jacobian matrix $J(a)$ has a pair of purely imaginary eigenvalues $\lambda = \pm i\omega_0$, where $\omega_0 = \sqrt{\frac{2\sigma^3}{(1+\sigma)^2}}$. Let $\lambda = \beta(a) \pm i\omega(a)$ be the roots of $\lambda^2 - \mathrm{Tr}(a)\lambda + \mathrm{Det}(a) = 0$, then

$$\beta(a) = \frac{\mathrm{Tr}(a)}{2}, \quad \omega(a) = \frac{\sqrt{4\mathrm{Det}(a) - \mathrm{Tr}^2(a)}}{2}.$$

Furthermore, we can verify

$$\beta'(a)|_{a=a_0} = \frac{\sigma}{4(1+\sigma)^2} > 0.$$

By the Poincaré-Andronov-Hopf bifurcation theorem (see [22, Theorem 3.1.3]), we know that (1.4) undergoes a Hopf bifurcation at (u_c, v_c) as a passes through a_0.

However, the detailed nature of the Hopf bifurcation needs further analysis of the normal form (see [23–25]) for model (1.4). To this end, we translate the equilibrium (u_c, v_c) to the origin by the translation $\tilde{u} = u - u_c$, $\tilde{v} = v - v_c$. For the sake of convenience, we still denote $\tilde{u}$ and $\tilde{v}$ by u and v, respectively. Thus, the local model (1.4) is transformed into

$$\begin{cases} \dfrac{\mathrm{d}u}{\mathrm{d}t} = \sigma(u + u_c)(1 - u - u_c) - (u + u_c)(1 + a(v - v_c))(v - v_c), \\ \dfrac{\mathrm{d}v}{\mathrm{d}t} = (u + u_c)(1 + a(v - v_c))(v - v_c) - (v - v_c). \end{cases} \tag{2.2}$$

Rewrite (2.2) as

$$\begin{pmatrix} \dfrac{\mathrm{d}u}{\mathrm{d}t} \\ \dfrac{\mathrm{d}v}{\mathrm{d}t} \end{pmatrix} = J(a)\begin{pmatrix} u \\ v \end{pmatrix} + \begin{pmatrix} f(u, v, a) \\ g(u, v, a) \end{pmatrix}, \tag{2.3}$$

where

$$f(u, v, a) = -auv^2 - \sigma u^2 - au_c v^2 - (1 + 2av_c)uv,$$

$$g(u, v, a) = auv^2 + au_c v^2 + (1 + 2av_c)uv.$$

Choose $\xi = (i\omega_0 - au_c v_c, (1 + av_c)v_c)^T$ as one of the eigenvectors of $J(a)$ corresponding to $i\omega_0$. Let

$$P = \begin{pmatrix} \omega_0 & -au_c v_c \\ 0 & (1 + av_c)v_c \end{pmatrix},$$

then

$$P^{-1} = \begin{pmatrix} \dfrac{1}{\omega_0} & \dfrac{au_c}{\omega_0(1 + av_c)} \\ 0 & \dfrac{1}{(1 + av_c)v_c} \end{pmatrix}.$$

The transformation $\begin{pmatrix} u \\ v \end{pmatrix} = P\begin{pmatrix} x \\ y \end{pmatrix}$ changes (2.3) into

$$\begin{pmatrix} \dfrac{\mathrm{d}x}{\mathrm{d}t} \\ \dfrac{\mathrm{d}y}{\mathrm{d}t} \end{pmatrix} = P^{-1}J(a)P\begin{pmatrix} x \\ y \end{pmatrix} + P^{-1}\begin{pmatrix} f(P(x, y)^T) \\ g(P(x, y)^T) \end{pmatrix} = \begin{pmatrix} 0 & -\omega_0 \\ \omega_0 & 0 \end{pmatrix}\begin{pmatrix} x \\ y \end{pmatrix} + \begin{pmatrix} f^1(x, y, a) \\ g^1(x, y, a) \end{pmatrix}, \tag{2.4}$$

where

$$
\begin{aligned}
f^1(x,y,a) &= \frac{1}{\omega_0} f(\omega_0 x - au_c v_c y, (1+av_c)v_c y) + \frac{au_c}{\omega_0(1+av_c)} g(\omega_0 x - au_c v_c y, (1+av_c)v_c y) \\
&= (a^2u_c v_c^2(av_c+1) - av_c^2(av_c+1)^2)xy^2 + (a^2v_c^2 + 2av_c + 1 - a^2u_c v_c - au_c)\frac{a^2u_c v_c^3}{\omega_0} y^3 \\
&\quad - \sigma\omega_0 x^2 + \left(\frac{au_c v_c(2a^2v_c^2 + 3av_c + 1)}{av_c+1} + 2a\sigma u_c v_c - 2a^2v_c^3 - 3av_c^2 - v_c\right)xy \\
&\quad + (av_c^2 + v_c - \sigma u_c - au_c v_c)\frac{a^2u_c v_c^2}{\omega_0} y^2, \\
g^1(x,y,a) &= \frac{1}{(1+av_c)v_c} g(\omega_0 x - au_c v_c y, (1+av_c)v_c y) \\
&= av_c\omega_0(av_c+1)xy^2 - a^2u_c v_c^2(av_c+1)y^3 + \frac{\omega_0}{av_c+1}(2a^2v_c^2 + 3av_c + 1)xy - a^2u_c v_c^2 y^2.
\end{aligned}
$$

So, the stability of Hopf bifurcation for model (1.4) at (u_c, v_c) is determined by the sign of the following quantity:

$$
\delta(a_0) := \frac{1}{16}(f^1_{xxx} + g^1_{xxy} + f^1_{xyy} + g^1_{yyy}) + \frac{1}{16\omega_0}(f^1_{xy}(f^1_{xx} + f^1_{yy}) - g^1_{xy}(g^1_{xx} + g^1_{yy}) - f^1_{xx}g^1_{xx} + f^1_{yy}g^1_{yy}),
$$

where all the partial derivatives are evaluated at the bifurcation point $(x, y, a) = (0, 0, a_0)$.

After calculation, we have

$$
\begin{aligned}
f^1_{xxx} &= f^1_{xxy} = g^1_{xxx} = g^1_{xxy} = 0, \quad f^1_{xyy} = -2\sigma^2(\sigma - 1), \quad f^1_{yyy} = \frac{6\sigma^3(\sigma-1)}{(\sigma+1)\omega_0}, \\
g^1_{xyy} &= 2\sigma(\sigma+1)\omega_0, \qquad g^1_{yyy} = -6\sigma^2, \qquad f^1_{xx} = -2\sigma\omega_0, \qquad f^1_{xy} = -\frac{\sigma(2\sigma^2 - 3\sigma - 1)}{\sigma+1}, \\
f^1_{yy} &= \frac{2\sigma^3(\sigma-2)}{(\sigma+1)^2\omega_0}, \qquad g^1_{xx} = 0, \qquad g^1_{xy} = (2\sigma+1)\omega_0, \qquad g^1_{yy} = -\frac{2\sigma^2}{\sigma+1}.
\end{aligned}
$$

Then

$$
\delta(a_0) = -\frac{1}{16}\sigma(3\sigma+2) < 0.
$$

By [26, Chapter 3] and $\beta'(a_0) > 0$, $\delta(a_0) < 0$, we summarize our results as follows.

Theorem 2.1. *Suppose that $\sigma > 0$, $a > \frac{1}{\sigma}$, and $a_0 = \frac{(1+\sigma)^2}{\sigma}$.*

(i) *The equilibrium (u_c, v_c) of model (1.4) is locally stable when $a < a_0$, and unstable when $a > a_0$;*
(ii) *Model (1.4) undergoes a Hopf bifurcation at (u_c, v_c) when $a = a_0$, the direction of the Hopf bifurcation is supercritical and the bifurcating periodic solutions are orbitally asymptotically stable.*

3 Dynamics of the diffusion model

For simplicity, in this section, we take the spatial domain Ω of model (1.5) as the one-dimensional interval $\Omega = (0, \pi)$.

3.1 Local stability analysis and Turing instability

Let $\tilde{u} = u - u_c$, $\tilde{v} = v - v_c$, we still denote $\tilde{u}$ and $\tilde{v}$ by u and v, respectively, and then the linearized system of (1.5) at (u_c, v_c) is written as follows:

$$\begin{pmatrix} u_t \\ v_t \end{pmatrix} = \begin{pmatrix} d_1\frac{\partial^2 u}{\partial x^2} - \sqrt{\frac{\sigma}{a}} & \frac{-2\sqrt{a\sigma}+1}{\sqrt{a\sigma}} \\ \frac{\sqrt{a\sigma}(\sqrt{a\sigma}-1)}{a} & d_2\frac{\partial^2 v}{\partial x^2} + \frac{\sqrt{a\sigma}-1}{\sqrt{a\sigma}} \end{pmatrix}\begin{pmatrix} u \\ v \end{pmatrix} =: L(a)\begin{pmatrix} u \\ v \end{pmatrix}, \tag{3.1}$$

with the Neumann boundary conditions

$$u_x(0,t) = v_x(0,t) = u_x(\pi,t) = v_x(\pi,t) = 0. \tag{3.2}$$

By [27, p. 602], it is easy to see that systems (3.1) and (3.2) have solution (u, v) formally written as

$$\begin{pmatrix} u(x,t) \\ v(x,t) \end{pmatrix} = \sum_{k=0}^{\infty}\begin{pmatrix} a_k \\ b_k \end{pmatrix} e^{\lambda t}\cos kx. \tag{3.3}$$

By substituting (3.3) into (3.1), we derive

$$\sum_{k=0}^{\infty}\begin{pmatrix} a_k \\ b_k \end{pmatrix}\lambda e^{\lambda t}\cos kx = \sum_{k=0}^{\infty}\begin{pmatrix} d_1\frac{\partial^2 u}{\partial x^2} - \sqrt{\frac{\sigma}{a}} & \frac{-2\sqrt{a\sigma}+1}{\sqrt{a\sigma}} \\ \frac{\sqrt{a\sigma}(\sqrt{a\sigma}-1)}{a} & d_2\frac{\partial^2 v}{\partial x^2} + \frac{\sqrt{a\sigma}-1}{\sqrt{a\sigma}} \end{pmatrix}\begin{pmatrix} a_k \\ b_k \end{pmatrix} e^{\lambda t}\cos kx.$$

We then equate powers of k, and in that way, one has

$$(\lambda I - J_k(a))\begin{pmatrix} a_k \\ b_k \end{pmatrix} = \begin{pmatrix} 0 \\ 0 \end{pmatrix}, \quad k = 0, 1, 2, \ldots, \tag{3.4}$$

where

$$J_k(a) = \begin{pmatrix} -d_1k^2 - \sqrt{\frac{\sigma}{a}} & \frac{-2\sqrt{a\sigma}+1}{\sqrt{a\sigma}} \\ \frac{\sqrt{a\sigma}(\sqrt{a\sigma}-1)}{a} & -d_2k^2 + \frac{\sqrt{a\sigma}-1}{\sqrt{a\sigma}} \end{pmatrix}.$$

So, system (3.4) has a nonzero solution $(a_k, b_k)^T$ if and only if

$$\mathrm{Det}(\lambda I - J_k(a)) = 0.$$

Rewrite it into the equation $\lambda^2 - T_k(a)\lambda + D_k(a) = 0$, where

$$T_k(a) = -(d_1 + d_2)k^2 + \frac{\sqrt{a\sigma} - 1 - \sigma}{\sqrt{a\sigma}}, \tag{3.5}$$

$$\begin{aligned} D_k(a) &= \left(-d_1k^2 - \sqrt{\frac{\sigma}{a}}\right)\left(-d_2k^2 + \frac{\sqrt{a\sigma}-1}{\sqrt{a\sigma}}\right) + \frac{(\sqrt{a\sigma}-1)(2\sqrt{a\sigma}-1)}{a} \\ &= \frac{2(\sqrt{a\sigma}-1)^2}{a} + d_1\left(d_2k^2 - \frac{\sqrt{a\sigma}-1}{\sqrt{a\sigma}}\right)k^2 + d_2\sqrt{\frac{\sigma}{a}}k^2. \end{aligned} \tag{3.6}$$

Under condition $a < a_0 = \frac{(1+\sigma)^2}{\sigma}$ we have $T_k(a) < 0$ for all $k = 0, 1, 2, \ldots$ and $D_0(a) > 0$. Let

$$r_m = \min_{1 \le k \le m} \frac{\frac{2(\sqrt{a\sigma}-1)^2}{a} + d_2\sqrt{\frac{\sigma}{a}}k^2}{\left(\frac{\sqrt{a\sigma}-1}{\sqrt{a\sigma}} - d_2k^2\right)k^2}.$$

If $\frac{\sqrt{a\sigma}-1}{d_2\sqrt{a\sigma}} \le 1$ or $m^2 < \frac{\sqrt{a\sigma}-1}{d_2\sqrt{a\sigma}} \le (m+1)^2$ and $d_1 < r_m$, then $D_k(a) \ge D_0(a) > 0$, so (u_c, v_c) is linearly stable for system (1.5). If $m^2 < \frac{\sqrt{a\sigma}-1}{d_2\sqrt{a\sigma}} \le (m+1)^2$ and $d_1 > r_m$, then there exists at least one negative in $D_1(a), \ldots, D_m(a)$, and so (u_c, v_c) is unstable for (1.5). Then, we can summarize the above discussion.

Theorem 3.1. *Suppose that* $a < a_0 = \frac{(1+\sigma)^2}{\sigma}$ *so that* (u_c, v_c) *is a locally stable equilibrium for* (1.4). *Then* (u_c, v_c) *is an unstable equilibrium of* (1.5) *if*

$$(H1)\quad m^2 < \frac{\sqrt{a\sigma} - 1}{d_2\sqrt{a\sigma}} \le (m+1)^2 \quad and \quad d_1 > r_m;$$

and (u_c, v_c) *is a locally stable equilibrium of* (1.5) *if*

$$(H2)\quad \frac{\sqrt{a\sigma} - 1}{d_2\sqrt{a\sigma}} \le 1,$$

or

$$(H3)\quad m^2 < \frac{\sqrt{a\sigma} - 1}{d_2\sqrt{a\sigma}} \le (m+1)^2 \quad and \quad d_1 < r_m,$$

where

$$r_m = \min_{1\le k\le m} \frac{\frac{2(\sqrt{a\sigma}-1)^2}{a} + d_2\sqrt{\frac{\sigma}{a}}k^2}{\left(\frac{\sqrt{a\sigma}-1}{\sqrt{a\sigma}} - d_2k^2\right)k^2}.$$

3.2 Hopf bifurcation

By (3.5) and (3.6) one can derive that $T_0(a_0) = 0, D_0(a_0) > 0$ and $T_j(a_0) < 0, D_j(a_0) > 0$ for all $j \in N$. This reveals that $a = a_0$ is a Hopf bifurcation point of model (1.5) at (u_c, v_c) and the corresponding Hopf bifurcation is spatially homogeneous. Note that the spatially homogeneous Hopf bifurcation of model (1.5) at (u_c, v_c) is in fact one of the ODE dynamics (1.4) at the equilibrium (u_c, v_c), see [27–29]. Therefore, by combining the analysis in Section 2, we can immediately reach the following result without any tedious calculations.

Theorem 3.2. *Suppose that* $\sigma > 0$, $a > \frac{1}{\sigma}$, *and* $a_0 = \frac{(1+\sigma)^2}{\sigma}$. *Then, model* (1.5) *undergoes a Hopf bifurcation at* (u_c, v_c) *when* $a = a_0$. *Moreover,*

(*i*) *If* (*H1*) *is satisfied, then the direction of the Hopf bifurcation is subcritical and the bifurcating periodic solutions are unstable*;

(*ii*) *If* (*H2*) *or* (*H3*) *is satisfied, then the direction of the Hopf bifurcation is supercritical and the bifurcating periodic solutions are orbitally asymptotically stable.*

Remark 3.1. Note that the existence of the spatially inhomogeneous periodic solutions to model (1.5) has been obtained in [14, Section 3], and these bifurcating periodic solutions are clearly unstable since the steady state (u_c, v_c) is unstable.

4 Numerical simulations

In this section, we present some numerical simulations to illustrate our theoretical analysis.

The local model (1.4) involves two parameters a, σ. First, choosing parameter $\sigma = 1$, we have the critical point $a_0 = 4$. By Theorem 2.1(i), we know the equilibrium $\left(\frac{1}{\sqrt{3}}, \frac{\sqrt{3}-1}{3}\right)$ is locally stable when $a = 3 < a_0$ (see Figure 1). From Theorem 2.1(ii), a Hopf bifurcation occurs at $a = 4.1 > a_0$, the direction of the bifurcation is supercritical and the bifurcating periodic solutions are asymptotically stable (Figure 2).

Take parameters as $a = 2, \sigma = 1, d_1 = 1, d_2 = 0.5$, then $a < a_0 = 4$ and (H2) are satisfied; the equilibrium $(u_c, v_c) = \left(\frac{1}{\sqrt{2}}, \frac{\sqrt{2}-1}{2}\right)$ is still stable under diffusive effects (Figure 3). Initial values are chosen as $u(x, 0) = 0.75 + 0.001\,\mathrm{rand}(1)$, $v(x, 0) = 0.2 + 0.001\,\mathrm{rand}(1)$.

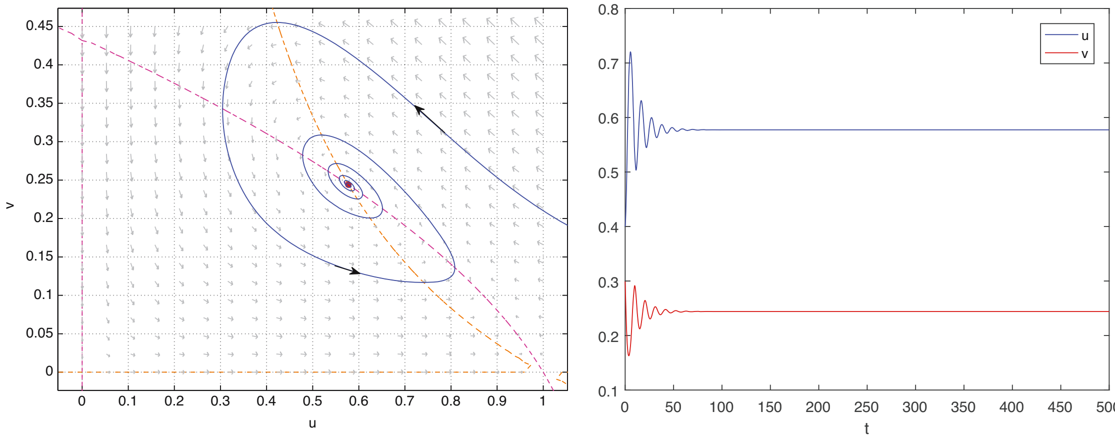

Figure 1: Phase portraits of model (1.4) with parameter $\sigma = 1$, the equilibrium $\left(\frac{1}{\sqrt{3}}, \frac{\sqrt{3}-1}{3}\right)$ is locally stable, where $a = 3 < a_0$.

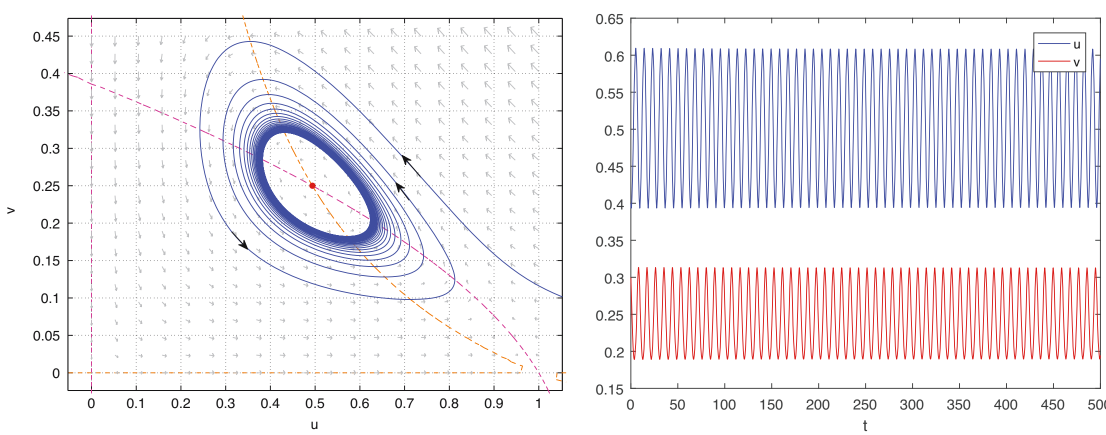

Figure 2: Phase portraits of model (1.4) with parameter $\sigma = 1$, the bifurcating periodic solution is stable, where $a = 4.1 > a_0$.

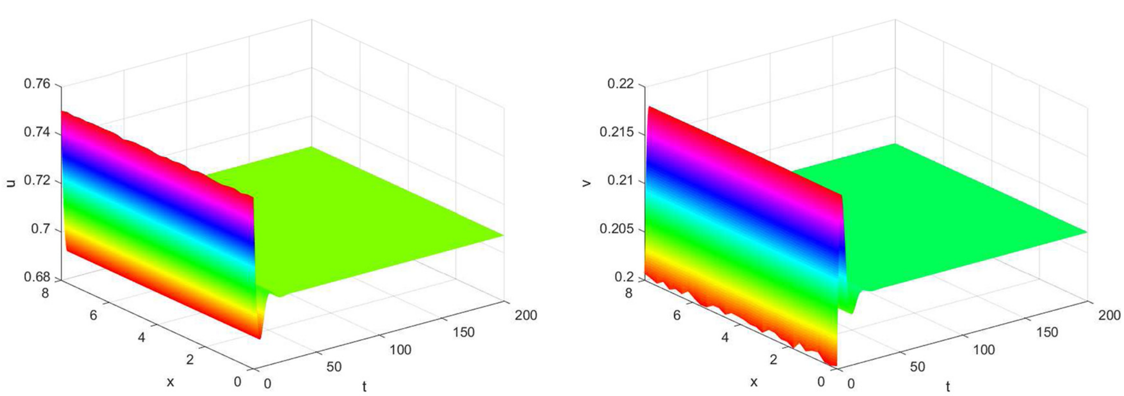

Figure 3: Phase portraits of (1.5) with parameters $a = 2$, $\sigma = 1$, $d_1 = 1$, $d_2 = 0.5$, the equilibrium $\left(\frac{1}{\sqrt{2}}, \frac{\sqrt{2}-1}{2}\right)$ is stable.

If the parameters are taken as $a = 2$, $\sigma = 1$, $d_1 = 2$, $d_2 = 0.2$, then $a < a_0 = 4$ and (H3) are satisfied, the equilibrium $(u_c, v_c) = \left(\frac{1}{\sqrt{2}}, \frac{\sqrt{2}-1}{2}\right)$ is still stable under diffusive effects (Figure 4). Initial values are chosen as $u(x, 0) = 0.75 + 0.001\,\mathrm{rand}(1)$, $v(x, 0) = 0.2 + 0.001\,\mathrm{rand}(1)$.

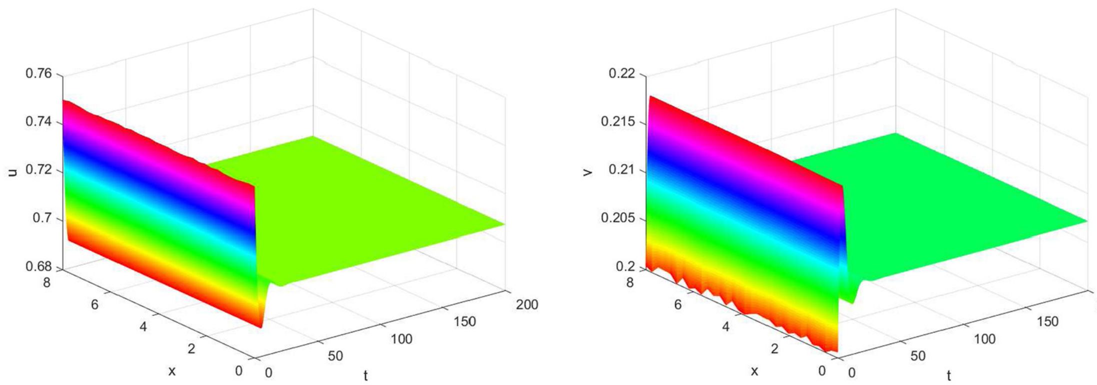

Figure 4: Phase portraits of (1.5) with parameters $a = 2$, $\sigma = 1$, $d_1 = 2$, $d_2 = 0.2$, the equilibrium $(\frac{1}{\sqrt{2}}, \frac{\sqrt{2}-1}{2})$ is stable.

However, when $a = 2$, $\sigma = 1$, $d_1 = 10$, $d_2 = 0.2$, then $a < a_0 = 4$ and (H1) are satisfied; the equilibrium $(u_c, v_c) = \left(\frac{1}{\sqrt{2}}, \frac{\sqrt{2}-1}{2}\right)$ becomes unstable under diffusive effects (Figure 5). Initial values are chosen as $u(x, 0) = 0.75 + 0.001\text{rand}(1)$, $v(x, 0) = 0.2 + 0.001\text{rand}(1)$.

Taking $a = 4.1$, $\sigma = 1$, $d_1 = 1$, $d_2 = 0.5$, then $a > a_0 = 4$ and (H2) are satisfied. In this case, theoretical analysis showed that the limit cycle from Hopf bifurcation is stable for (1.5). For numerical results, see Figure 6. Initial values are taken as $u(x, 0) = 0.75 + 0.2\text{rand}(1)$, $v(x, 0) = 0.2 + 0.2\text{rand}(1)$, close to the limit cycle.

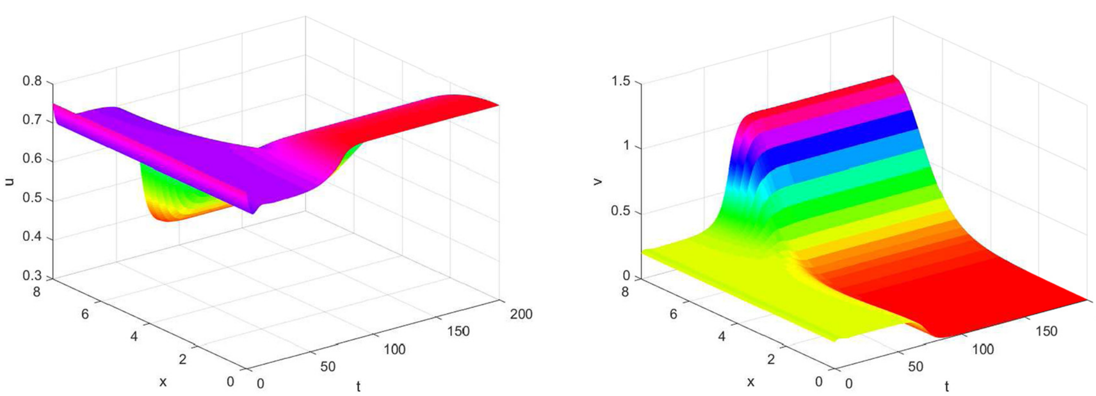

Figure 5: Phase portraits of (1.5) with parameters $a = 2$, $\sigma = 1$, $d_1 = 10$, $d_2 = 0.2$, the equilibrium $\left(\frac{1}{\sqrt{2}}, \frac{\sqrt{2}-1}{2}\right)$ becomes unstable.

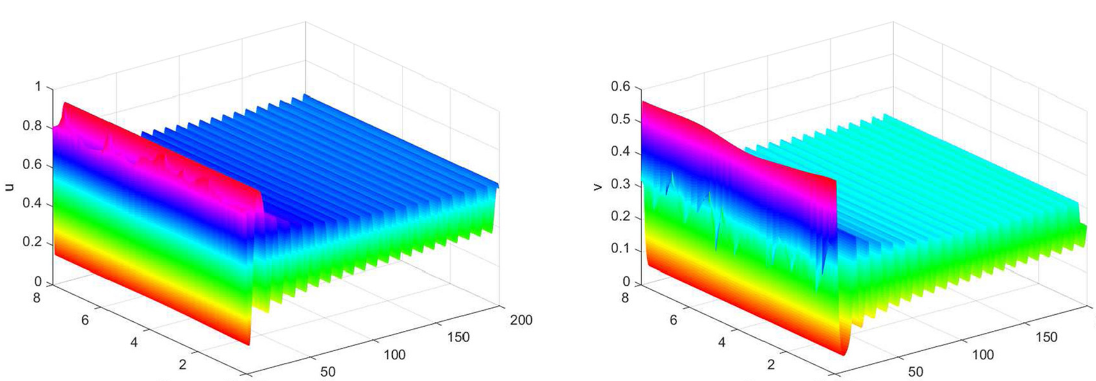

Figure 6: Phase portraits of (1.5) with parameters $a = 4.1$, $\sigma = 1$, $d_1 = 1$, $d_2 = 0.5$. Bifurcated homogeneous periodic solution is stable.

The similar phenomenon occurs when parameters are taken as $a = 4.1$, $\sigma = 1$, $d_1 = 2$, $d_2 = 0.2$, then $a > a_0 = 4$ and (H3) are satisfied. In this case, the limit cycle from Hopf bifurcation is stable for (1.5) (Figure 7). Initial values are taken as $u(x, 0) = 0.75 + 0.2\text{rand}(1)$, $v(x, 0) = 0.2 + 0.2\text{rand}(1)$, close to the limit cycle.

When parameters are taken as $a = 4.1$, $\sigma = 1$, $d_1 = 10$, $d_2 = 0.2$, then $a > a_0 = 4$ and (H1) are satisfied. In this case, the limit cycle from Hopf bifurcation is unstable for (1.5). Numerical results are shown in Figure 8. Initial values are taken as $u(x, 0) = 0.75 + 0.2\text{rand}(1)$, $v(x, 0) = 0.2 + 0.2\text{rand}(1)$.

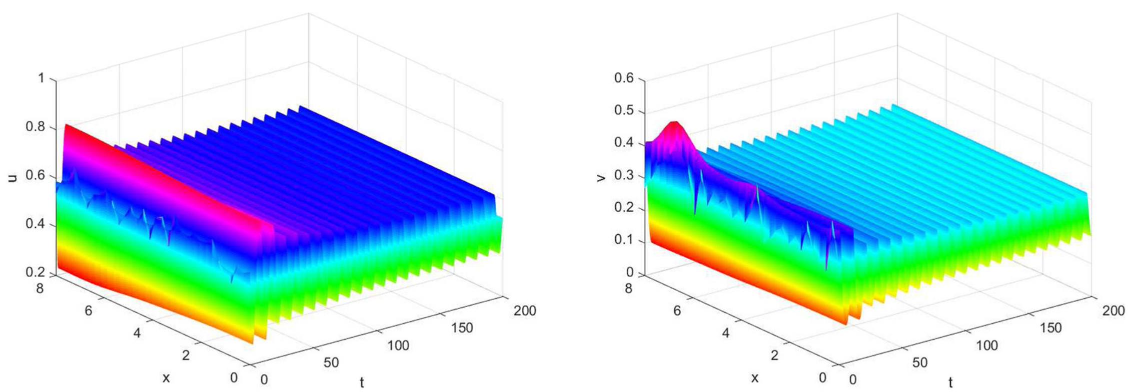

Figure 7: Phase portraits of (1.5) with parameters $a = 4.1$, $\sigma = 1$, $d_1 = 2$, $d_2 = 0.2$. Bifurcated homogeneous periodic solution is stable.

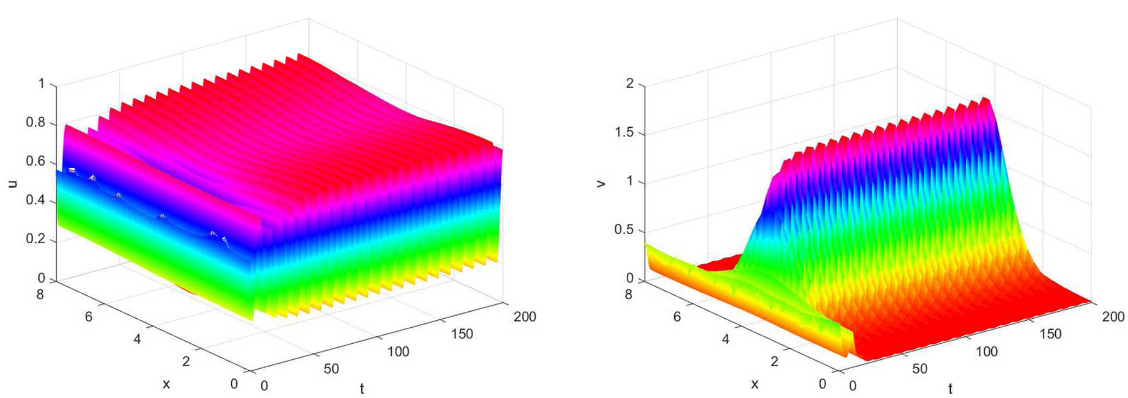

Figure 8: Phase portraits of (1.5) with parameters $a = 4.1$, $\sigma = 1$, $d_1 = 10$, $d_2 = 0.2$. Bifurcated homogeneous periodic solution is unstable.

5 Conclusion

In this article, we study the diffusive predator-prey model (1.5) with hunting cooperation under Neumann boundary conditions. The predator cooperation in hunting rate a plays a key role in determining the dynamics of the model. We provide detailed analyses of the Hopf Bifurcation and Turing instability in model (1.5) via three possible mechanisms: (i) For the local model of (1.5), we analyzed the stability of the equilibrium and derived conditions for determining the direction of Hopf bifurcation and the stability of the bifurcating periodic solution by the center manifold and the normal form theory (see Theorem 2.1). Our result showed that hunting cooperation could be beneficial to the predator population. (ii) We studied the Turing instability of the reaction-diffusion model (1.5) when the spatial domain is a bounded interval (see Theorem 3.1). Our result showed that hunting cooperation might be one of the determining factors in producing Turing patterns. In fact, we can find that Turing instability never occurs in model (1.5) without hunting cooperative. (iii) Combining the analysis of (i) and (ii), we immediately reach the direction and stability of the Hopf bifurcation for model (1.5) without any tedious calculations (see Theorem 3.2). Moreover, numerical simulations are also carried out to illustrate theoretical analysis, from which the theoretical results are verified. More interesting and complex behavior of such models will further be explored.

Acknowledgements: The authors would like to thank the referees for their very careful reading of the manuscript and valuable comments.

Funding information: This work is supported by the High-level talent program of QHMU (No. 2021XJG10) and the Natural Science Foundation of Qinghai Province (2021-ZJ-957Q).

Author contributions: LYM completed the main study and wrote the manuscript, ZQH checked the proofs process and verified the calculation. Moreover, all the authors read and approved the last version of the manuscript.

Conflict of interest: All of the authors of this article claim that together they have no competing interests.

Data availability statement: Not applicable.

References

[1] A. Lotka, *Undamped oscillations derived from the law of mass action*, J. Amer. Chem. Soc. **42** (1920), 1595–1599, DOI: https://doi.org/10.1021/ja01453a010.

[2] V. Volterra, *Fluctuation in the abundance of a species considered mathematically*, Nature **118** (1926), 558–560, DOI: https://doi.org/10.1038/118558a0.

[3] I. Bailey, J. Myatt, and A. Wilson, *Group hunting within the carnivora: physiological, cognitive and environmental influences on strategy and cooperation*, Behav. Ecol. Sociobiol. **67** (2013), 1–17, DOI: https://doi.org/10.1007/s00265-012-1423-3.

[4] D. Macdonald, *The ecology of carnivore social behaviour*, Nature **301** (1983), 379–384, DOI: https://doi.org/10.1038/301379a0.

[5] C. Packer, D. Scheel, and A. Pusey, *Why lions form groups: food is not enough*, Am. Nat. **136** (1990), no. 1, 1–19, DOI: https://doi.org/10.1086/285079.

[6] P. Schmidt and L. Mech, *Wolf pack size and food acquisition*, Am. Nat. **150** (1997), no.4, 513–517, DOI: https://doi.org/10.1086/286079.

[7] S. Creel and N. Creel, *Communal hunting and pack size in African wild dogs*, *Lycaon Pictus*. Anim. Behav. **50** (1995), 1325–1339, DOI: https://doi.org/10.1016/0003-3472(95)80048-4.

[8] C. Boesch, *Cooperative hunting in wild chimpanzees*, Anim. Behav. **48** (1994)653–667, DOI: https://doi.org/10.1006/anbe.1994.1285.

[9] D. Hector, *Cooperative hunting and its relationship to foraging success and prey size in an avian predator*, Ethology **73** (2010), no. 3, 247–257, DOI: https://doi.org/10.1111/j.1439-0310.1986.tb00915.x.

[10] M. Moffett, *Foraging dynamics in the group-hunting myrmicine ant, Pheidologeton diversus*, J. Insect Behav. **1** (1988), no. 3, 309–331, DOI: https://doi.org/10.1007/BF01054528.

[11] G. Uetz, *Foraging strategies of spiders*, Trends Ecol. Evol. **7** (1992), no. 5, 155–159, DOI: https://doi.org/10.1016/0169-5347(92)90209-T.

[12] L. Berec, *Impacts of foraging facilitation among predators on predator-prey dynamics*, Bull. Math. Biol. **72** (2010), no. 1, 94–121, DOI: https://doi.org/10.1007/s11538-009-9439-1.

[13] M. Alves and F. Hilker, *Hunting cooperation and Allee effects in predators*, J. Theoret. Biol. **419** (2017), 13–22, DOI: https://doi.org/10.1016/j.jtbi.2017.02.002.

[14] D. Wu and M. Zhao, *Qualitative analysis for a diffusive predator-prey model with hunting cooperative*, Phys. A **515** (2019), 299–309, DOI: https://doi.org/10.1016/j.physa.2018.09.176.

[15] A. Turing, *The chemical basis of morphogenesis*, Philos. Trans. R. Soc. B **237** (1952), 37–72, DOI: https://doi.org/10.1007/BF02459572.
[16] F. Capone, M. Carfora, R. De Luca, and I. Torcicollo, *Turing patterns in a reaction-diffusion system modeling hunting cooperation*, Math. Comput. Simulation **165** (2019), 172–180, DOI: https://doi.org/10.1016/j.matcom.2019.03.010.
[17] T. Singh and R. Dubey, *Pattern formation dynamics of predator-prey system with hunting cooperation in predators*, Math. Eng. **6** (2019), 245–276, DOI: https://doi.org/10.1201/b22521-9.
[18] D. Song, C. Li, and Y. Song, *Stability and cross-diffusion-driven instability in a diffusive predator-prey system with hunting cooperation functional response*, Nonlinear Anal. Real World Appl. **54** (2020), 103106, DOI: https://doi.org/10.1016/j.nonrwa.2020.103106.
[19] P. Saheb, H. Mainul, P. Pijush, N. Pati, P. Nikhil, and C. Joydev, *Cooperation delay induced chaos in an ecological system*, Chaos **30** (2020), no. 8, 083124, DOI: https://doi.org/10.1063/5.0012880.
[20] N. Pati, G. Layek, and N. Pal, *Bifurcations and organized structures in a predator-prey model with hunting cooperation*, Chaos Solitons Fractals **140** (2020), 110184, DOI: https://doi.org/10.1016/j.chaos.2020.110184.
[21] Y. Chou, Y. Chow, X. Hu, and R. Jang, *A ricker type predator-prey system with hunting cooperation in discrete time*, Math. Comput. Simulation **190** (2021), 570–586, DOI: https://doi.org/10.1016/j.matcom.2021.06.003.
[22] S. Wiggins, *Introduction to Applied Nonlinear Dynamical Systems and Chaos*, Springer, New York, 1991.
[23] G. Layek and N. Pati, *Period-bubbling transition to chaos in thermo-viscoelastic fluid systems*. Internat. J. Bifur. Chaos Appl. Sci. Engrg. **30** (2020), no. 6, 2030013, DOI: https://doi.org/10.1142/S021812742030013X.
[24] G. Layek and N. Pati, *Bifurcations and hyperchaos in magnetoconvection of non-Newtonian fluids*. Internat. J. Bifur. Chaos Appl. Sci. Engrg. **28** (2018), no. 10, 1830034, DOI: https://doi.org/10.1142/S0218127418300343.
[25] G. Layek, *An Introduction to Dynamical Systems and Chaos*, Springer-Verlag, New York, 2015.
[26] J. Guckenheimer and P. Holmes, *Nonlinear Oscillations, Dynamical Systems, and Bifurcations of Vector Fields*, Springer-Verlag, New York, 1983.
[27] R. Wu, Y. Zhou, Y. Shao, and L. Chen, *Bifurcation and Turing patterns of reaction-diffusion activator-inhibitor model*, Phys. A **482** (2017), 597–610, DOI: https://doi.org/10.1016/j.physa.2017.04.053.
[28] F. Yi, J. Wei, and J. Shi, *Diffusion-driven instability and bifurcation in the Lengyel-Epstein system*, Nonlinear Anal. Real World Appl. **9** (2008), no. 3, 1038–1051, DOI: https://doi.org/10.1016/j.nonrwa.2007.02.005.
[29] X. Yan and C. Zhang, *Turing instability and formation of temporal patterns in a diffusive bimolecular model with saturation law*, Nonlinear Anal. Real World Appl. **43** (2018), 54–77, DOI: https://doi.org/10.1016/j.nonrwa.2018.02.004.